Available online at www.sciencedirect.com
ScienceDirect
Surface & Coatings Technology 201 (2007) 8799–8807
SURFACE & COATINGS TECHNOLOGY
www.elsevier.com/locate/surfcoat

Spatial control over atomic layer deposition using microcontact-printed resists

Xirong Jiang [a], Rong Chen [b,1], Stacey F. Bent [c,*]

[a] Department of Physics, Stanford University, Stanford, California 94305, USA
[b] Department of Chemistry, Stanford University, Stanford, California 94305, USA
[c] Department of Chemical Engineering, Stanford University, Stanford, California 94305, USA

Received 12 April 2007; accepted in revised form 27 April 2007
Available online 10 May 2007

Abstract

Area-selective thin film growth by atomic layer deposition (ALD) has been achieved on octadecyltrichlorosilane (ODTS) patterned substrates. Patterned hydrophobic self-assembled monolayers (SAMs) were first transferred to silicon and yttria-stabilized zirconia (YSZ) substrates by microcontact printing. Subsequently, films of either HfO_2 or Pt were grown selectively on the SAM-free regions of the surface, while ALD was blocked in regions where ODTS was present. The deposited pattern was readily observed through scanning electron microscopy and scanning Auger imaging, demonstrating that soft lithography is a simple and promising method to achieve area-selective ALD. The selectivity of the soft lithography-based method and the subsequent pattern resolution was compared for Pt versus HfO_2. It was found that using ODTS films, it is easier to achieve complete deactivation of Pt than HfO_2.

Keywords: Platinum; Hafnium dioxide; Atomic layer deposition; Microcontact printing; Self-assembled monolayer

1. Introduction

Atomic layer deposition (ALD) is a powerful thin film growth technique that employs a sequence of self-limiting surface reaction steps to afford sub-nanometer control of the growth process [1–5]. The self-limiting adsorption reactions ensure the precise control of film thickness, conformality, and uniformity over large area. Typically, the process permits nanoscale control in the vertical direction. To extend the method to three dimensional control of materials, we have been investigating area-selective ALD techniques which will enable micro- and ultimately nano-scale definition of the lateral structure for 3D patterning. Area-selective ALD differs from conventional, subtractive lithographic patterning: it is an additive process in which material is deposited only where needed [6–13].

Our group has investigated different patterning methods for implementing the area-selective ALD process, including photolithographically-patterned SiO_2/Si substrates [7,14], direct writing by electron and photon beams [15], and soft lithography [16,17]. Here we review our recent results on area-selective ALD using soft lithography, and compare the degree of selectivity achieved for two different deposited materials. We show that good spatial control over atomic layer deposition can be achieved using microcontact-printed resists.

We have carried out area-selective ALD using soft lithography for both a metal oxide (HfO_2) and a metal (Pt). HfO_2 was chosen due to its importance in microelectronics applications. As the lateral dimensions of metal oxide-semiconductor field-effect transistors (MOSFETs) continue decreasing and higher switching speeds are required, the thickness of the SiO_2 gate dielectrics must be substantially decreased to a few atomic layers. However, the leakage current caused by direct electron tunneling from the gate to the channel increases exponentially with decreasing dielectric thickness

* Corresponding author. Department of Chemical Engineering, Stanford University, Stanford, California 94305, USA. Tel.: +1 650 723 0385; fax: +1 650 723 9780.
E-mail address: sbent@stanford.edu (S.F. Bent).
[1] Current address: Applied Materials, 974 E. Arques Ave. M/S 81305, Sunnyvale, CA 94086, USA.

0257-8972/$ - see front matter © 2007 Elsevier B.V. All rights reserved.
doi:10.1016/j.surfcoat.2007.04.126

[10,18]. In order to overcome this difficulty, gate dielectrics with permittivities greater than that of SiO_2, such as HfO_2, are required [19]. High-k dielectric layers allow deposition of thicker layers while retaining the same effective oxide thickness.

Pt has enormous application prospects in both catalysis and microelectronics [20,21]. For example, due to its chemical stability in both oxidative and reductive environments, and its excellent electrical properties at high temperatures [22], Pt is used as the electrode material in nonvolatile ferroelectric random access memory devices and high dielectric capacitors. It also exhibits excellent catalytic activity for a number of reactions, including the O_2 reduction reaction at the cathode of a solid oxide fuel cell (SOFC), and is especially useful at the lower operating temperatures (below 600 °C) that are desired for integratable fuel cell systems [23].

Several groups have used microcontact-printed (μCP) resists for selective ALD of films such as TiO_2, ZnO and Ru [9,11,13,24–26]. These resists have typically consisted of self-assembled monolayers (SAMs). SAMs are thin organic films which form spontaneously on solid surfaces, and are well known for modifying the physical, chemical, and electrical properties of semiconducting, insulating and metallic surfaces. Their potential applications include the control of wetting and adhesion, tribology, chemical sensing, ultra-fine scale lithography and protection of metals against corrosion [27–29]. In our area-selective ALD process, we used self-assembled monolayers made from octadecyltrichlorosilane (ODTS) to modify the chemical properties of the substrate surface. Due to the robust, covalent Si–O linkage between the molecules and the surface, films formed by ODTS demonstrate good chemical and thermal stability, and ODTS has been demonstrated as an efficient monolayer resist for a number of ALD processes [8,12].

The approach of using microcontact printing to achieve area-selective ALD consists of three key steps, as illustrated in Fig. 1. First, PDMS stamps are fabricated through standard lithographic methods and inked with ODTS precursors [30]. Second, the pattern encoded in the PDMS stamp is transferred via application of the SAM onto the substrate by microcontact printing. Third, HfO_2 or Pt thin films are selectively deposited by ALD onto areas of the substrate that are not deactivated by ODTS, and the ODTS resist is removed.

In this paper, we will show that patterned ODTS transferred onto the substrate by microcontact printing can reduce or prevent the atomic layer deposition of HfO_2 and Pt at the printed areas. Furthermore, we will compare the area selectivity and the subsequent resolution of the patterned HfO_2 and Pt fabricated through the soft lithography-based method. Finally, for the area-selective ALD of HfO_2, we will compare the selectivity and resolution of the soft lithography-based approach with the method based upon selective surface attachment on patterned SiO_2/Si.

2. Experimental

2.1. Chemical reagents

All chemical reagents, including octadecyltrichlorosilane (ODTS) (97%), toluene (anhydrous, 99.8%) and chloroform (99%), used to form SAMs were purchased from Aldrich (Milwaukee, WI) without further treatment. Poly(dimethylsiloxane) (PDMS) (Sylgard 184) was purchased from Dow Corning.

2.2. Substrates

All silicon sample pieces were cut from Si (100) wafers purchased from Si-Tech, Inc. (p-type with boron dopant; resistivity of 1.0–10.0 Ω cm). The wafer pieces were cleaned by sonication in chloroform, DI water rinsing, piranha etch, a second DI water rinsing, and finally blown dry with a N_2 flow. The result is a chemical oxide-coated silicon substrate. Thin film yttria-stabilized zirconia (YSZ) substrates, coated on Si (100), were provided by Friedrich Prinz's group at Stanford University. Two steps were used to clean the YSZ substrates [31]. First the substrates were rinsed ultrasonically, twice, for 5 min in ethyl alcohol in order to remove grease. After the first

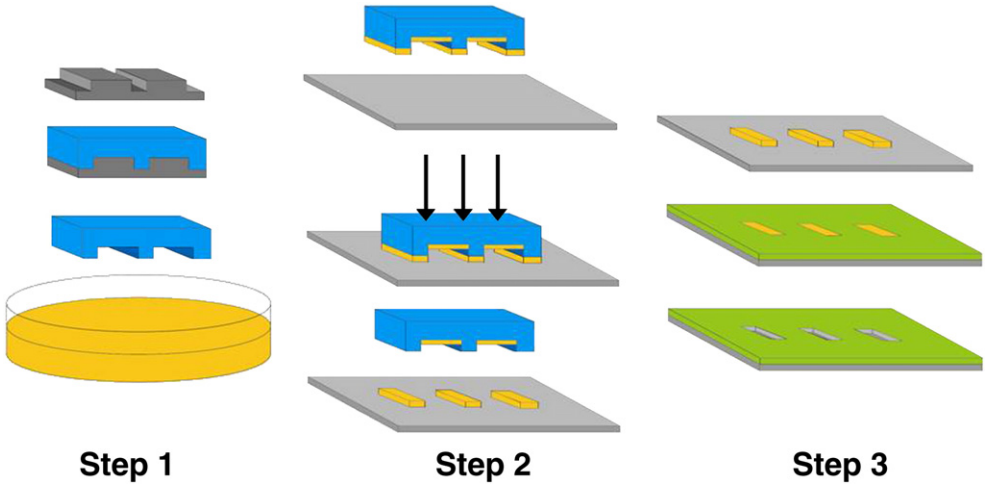

Fig. 1. Schematic outline of the procedure to fabricate patterned HfO_2 or Pt thin films using microcontact printing and selective atomic layer deposition.

rinse, the ethyl alcohol was renewed. Following the ethyl alcohol rinses, the YSZ substrates were exposed to RF oxygen plasma for 10 min to make the surface hydrophilic.

2.3. Preparation of unpatterned and patterned ODTS SAMs

All procedures for SAM formation were performed in a dry, air-purged glovebox at room temperature. Previous studies have shown that the deactivating effect of ODTS SAMs depends on its quality, and that densely packed SAMs are required for good deactivation [7,12,32]. To demonstrate the level of resistance of the SAMs against Pt and HfO_2 ALD, unpatterned (continuous) ODTS SAMs were formed from solution. For preparation of the unpatterned SAMs, the cleaned Si and YSZ substrates were dipped in 10 mM ODTS solutions in toluene without disturbance for times ranging from 5 min to 2 days. The unpatterned ODTS-coated samples were examined using water contact angle and ellipsometry measurements before loading them into the ALD reactor.

Patterned monolayers of ODTS on the Si and YSZ substrates were made using μCP. Masters were fabricated from patterned Si wafers by conventional photolithography. In the area-selective ALD process, the masters used for the HfO_2 and Pt experiments were of a hexagonal pillar structure and a mesh structure, respectively. The vertical scale for both types of masters was 7 μm. The lateral scales were 25 μm and 6 μm for the masters used for the HfO_2 and Pt systems, respectively. The stamps were fabricated by casting polydimethylsiloxane (PDMS) on the masters [30]. After curing, the PDMS stamps were peeled away from the masters. The resultant stamps were inked with the ODTS solution and were brought into contact with the Si or YSZ substrates. When the stamps are made from the masters, the raised parts of the master correspond to the recessed spaces of the stamps. When patterned SAMs of ODTS were made using these stamps, therefore, a negative, hydrophobic pattern of the original master was produced on the Si or YSZ substrate. Hence the hexagonal pillars on the master created hexagonal rings of ODTS on the substrate, while the grid-based master led to the transfer of squares of ODTS onto the substrate.

To prepare the patterned SAMs for the process of area-selective ALD, different contact times and weights were employed. The stamp was placed in contact with the substrates for 30 s under a 2 g weight for the HfO_2 process, and for 5 min under a 43 g weight for the Pt process. After the appropriate contact time, the stamp was carefully peeled off, and the substrate was rinsed by toluene, acetone, and chloroform sequentially, then finally dried by nitrogen flow. All the samples were stored in the glove box for more than 10 h before the analysis and subsequent experiments.

2.4. Atomic layer deposition process

The samples were loaded into custom built, flow-type ALD systems for the atomic layer deposition of HfO_2 and Pt thin films. The detailed ALD conditions for deposition of HfO_2 and Pt thin films, including the precursor dose times, the purge times, and the source and substrate temperatures can be found elsewhere [7,12,17,32,33]. For all the area-selective ALD experiments, the number of ALD cycles for the HfO_2 and Pt deposition are kept at 50 cycles and 100 cycles, respectively, which led to growth of 36–38 Å thickness HfO_2 films and 33–35 Å Pt films.

2.5. Analysis techniques

For unpatterned film deposition on a reference sample, the elemental composition of the HfO_2 and Pt films was measured by X-ray photoelectron spectroscopy (XPS) using Al Kα radiation with an X-ray monochromator. The HfO_2 film thickness was measured by ellipsometry and characterized by transmission electron microscopy (TEM). The Pt film thickness was measured by ellipsometry with prior calibration by X-ray reflectometry (XRR). For the patterned substrate, the topographic structure was viewed by scanning electron microscopy (SEM). The elemental analysis on the micropatterned regions was explored by Auger electron spectroscopy (AES), and elemental mapping and line scans were obtained with scanning Auger analysis carried out in the Evans Analytical Group. All of the spectra shown in this paper have a detection sensitivity of ~ 0.1at.%.

3. Results and discussion

3.1. Use of ODTS SAMs as ALD resists

In order to carry out area-selective ALD, a good resist system is needed to block the substrate surface active sites. The ODTS SAM was tested for resistance against ALD of both of HfO_2 and Pt. For ALD of HfO_2 thin films, two different Hf precursors – hafnium(IV)-tetrachloride ($HfCl_4$) and tetrakis(dimethylamido) hafnium(IV) ($Hf[N(CH_3)_2]_4$) – plus water have been employed. The HfO_2 ALD process includes two self-limiting chemical reactions, repeated in alternating ABAB sequences as shown below:

$$A: Hf\text{–}OH^* + HfCl_4 \rightarrow Hf\text{–}O\text{–}HfCl_3^* + HCl\uparrow$$

$$B: Hf\text{–}Cl^* + H_2O \rightarrow Hf\text{–}OH^* + HCl\uparrow,$$

or

$$A: Hf\text{–}OH^* + Hf[N(CH_3)_2]_4 \rightarrow Hf\text{–}O\text{–}Hf[N(CH_3)_2]_3^* + NH(CH_3)_2\uparrow$$

$$B: Hf\text{–}N(CH_3)_2^* + H_2O \rightarrow Hf\text{–}OH^* + NH(CH_3)_2\uparrow,$$

where the asterisks represent the surface species. Pt thin films were deposited onto Si and YSZ substrates using (methylcyclopentadienyl)trimethylplatinum ($MeCpPtMe_3$) and air, providing a source of oxygen, as ALD precursors. The growth

mechanism for Pt, proposed by Aaltonen et al. [34–36], includes two self-limiting chemical reactions,

$$A : Pt(s) + O_2 \rightarrow Pt\text{–}O^*$$

$$B : CH_3C_5H_4Pt(CH_3)_3 + Pt\text{–}O^* \rightarrow Pt(s) + CO_2(g)\uparrow + H_2(g)\uparrow + \text{other byproducts}\uparrow$$

A systematic study of the deactivating effect of octadecyltrichlorosilane (ODTS) SAMs toward both HfO_2 and Pt ALD was carried out. ODTS SAMs formed on silicon substrates by different dipping times were characterized by ellipsometry and water contact angle. The results are shown in Fig. 2. The film thickness of the ODTS SAM increased with SAM formation time until a plateau was reached at values of 26 Å; the contact angle was found to exhibit similar behavior, reaching a maximum value of 110°, which is consistent with previous reports [12,27,37,38]. The contact angle measurement reveals the hydrophobicity of the monolayer, and the change in the contact angle roughly indicates the extent of the monolayer surface coverage as well as the variation in the surface chemical composition of the substrate [39–42]. Approximately 2 h was required for the water contact angle of the ODTS SAM to reach a plateau, indicating that the formation of a closely packed monolayer takes at least 2 h.

Another set of ODTS-coated substrates prepared in the same process was introduced into the ALD reactor for 50 cycles of ALD HfO_2 or 100 cycles of ALD Pt. XPS studies of these substrates after the HfO_2 and Pt ALD process show that the Hf and Pt atomic percentages (Fig. 2) are negatively correlated with the contact angle and thickness of the monolayer resist. In other words, the more hydrophobic and the thicker the monolayer, the more resistance it exhibits against the ALD process for both HfO_2 and Pt.

It is interesting to compare the ODTS blocking effect on HfO_2 versus Pt ALD. Although the trend of the deactivation behavior is similar, it takes 48 h to fully block the HfO_2 ALD process while only 12 h is needed to fully block the Pt ALD growth. Thus, the Pt ALD growth is more easily deactivated by the SAM, as indicated by the absence of observable Pt on ODTS films with shorter silylation times. Here we speculate as to a possible reason for the difference between Pt and HfO_2. The explanation is based on the difference of the inherent chemical reactivity of the precursors used in the two processes. The ability to block ALD with shorter silylation times for the Pt process suggests that the Pt precursor and dry air may not be as reactive as hafnium precursor and water. In addition, the difference of oxygen affinity between the Hf and Pt may play a role here. In a study by Park et al. [9], Ru nucleation was also found to be less sensitive to the quality of the monolayer surface than deposition of Hf or Zr oxide [32] and Ti [43] based films. This effect was attributed to the lower oxygen affinity of Ru, making the ruthenium precursor less likely to penetrate the monolayer and react with oxide present at the silicon/monolayer interface [9]. A similar phenomenon may be occurring with Pt. Both of these arguments noted above support the conclusion that the conditions for blocking the Pt ALD are less stringent compared to those needed to block HfO_2 growth.

Once the applicability of ODTS as a resist was confirmed, patterned octadecylsiloxane SAMs were made on the Si and YSZ substrates using μCP. In this process the contact time was found to be important to the integrity of the pattern transfer. When the stamp was removed too quickly, loss of pattern resolution occurred, likely because the ODTS was still wet and spread. However, long contact times between the PDMS and the substrate sometimes resulted in the breakage of the PDMS stamp such that parts of the stamp remained on the substrate or on the stamp itself. Long contact time can also lead to loss of the pattern integrity when the "ink" starts spreading on the substrate. In our process, the contact times were optimized to

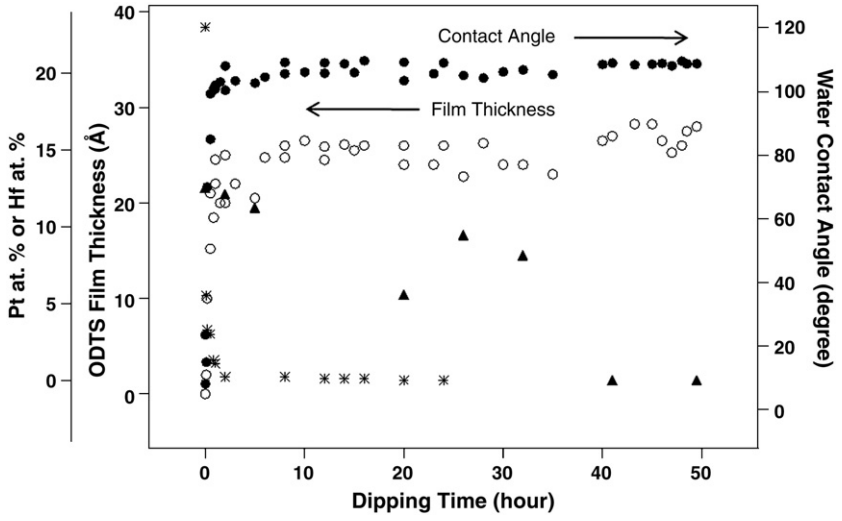

Fig. 2. Time dependence of ODTS film formation and its ALD blocking effectiveness on HfO_2 and Pt ALD, where the number of ALD cycles for the HfO_2 and Pt deposition are kept at 50 cycles and 100 cycles, respectively. Water contact angle measured on the ODTS film(●), ODTS film thickness (○), Hf at.% (▲) and Pt at.% (*).

be 30 s and 5 min for HfO_2 and Pt, respectively. Patterned octadecylsiloxane SAMs were fabricated on the Si and YSZ substrates using μCP with these optimal contact times for the following area-selective ALD processes.

3.2. Selective atomic layer deposition of HfO_2 and Pt thin films

In the atomic layer deposition of both HfO_2 or Pt films, the process strongly depends on the surface active sites. Once these sites are deactivated by the SAM layer, HfO_2 or Pt can, in principle, no longer be deposited on the deactivated areas and will deposit only on the areas free from the SAM. This procedure therefore provides a quick and relatively easy method for performing area-selective ALD. In contrast, other procedures, such as the selective-attachment based method [7] or other lithographic procedures [44–46] are more complicated and costly.

We first discuss area-selective ALD of HfO_2 using microcontact printing. After μCP using a stamp with hexagonal pillars, 36–38Å thick HfO_2 thin films were selectively deposited onto the patterned Si substrates. Subpanels (a) and (b) of Fig. 3 are SEM images of the printed area before and after HfO_2 ALD, while subpanels (c) and (d) of Fig. 3 are the results of AES analysis. It is clear that the hexagonal pattern structure has been successfully transferred to the substrate. In Fig. 3(a), the light hexagonal borders correspond to the ODTS film. The brighter contrast is due to both topographic and charging effects. After HfO_2 ALD, the reverse in image contrast in Fig. 3(b) suggests that HfO_2 has been deposited inside the hexagons. In the SEM image of Fig. 3(b), a horizontal line marks the location of the AES line scan analysis used to obtain the data in Fig. 3(c). The AES line scans, which are used to compare the relatively intensity of C and Hf as a function of position, show that the C and Hf spectra clearly alternate as expected.

Fig. 3(d) contains the hafnium elemental Auger mapping image, which was acquired by measuring the peak intensity of the hafnium as a function of beam position. The maps show the relative elemental distributions (peak intensity) as a pixel intensity; that is the greater the Auger peak intensity, the brighter the pixel value. The bright regions in Fig. 3(d) indicate the presence of Hf while the dark areas indicate the absence of Hf. Whereas the SEM image provides topographical information on the surface, the Auger mapping image reveals the spatial distribution of a specific element, in this case hafnium. The comparison of these two images demonstrates the same shape, which indicates some degree of confinement of the deposition to the non-printed areas.

However, it is noticeable that both the elemental mapping and line scan obtained by Auger analysis demonstrate an indistinct interface between deactivated regions and HfO_2 growth regions. Hafnium is observed on the edge/side of the hexagon, illustrated by the brighter spots in some area of the ODTS-coated regions. The growth of the undesired HfO_2 film can be attributed to the defects presented in the microcontact-printed ODTS layer. It takes 48 h to form from the solution phase a

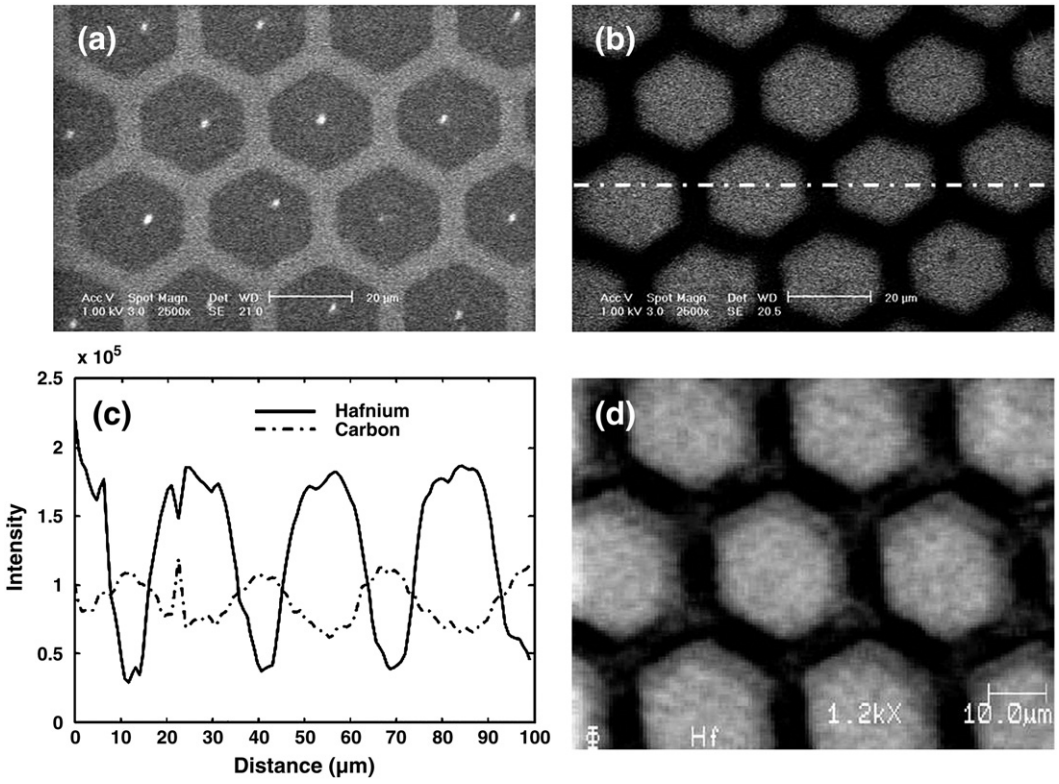

Fig. 3. SEM image of microcontact printing patterned area (a) before and (b) after ALD HfO_2; AES analysis on patterned structure after the area-selective ALD of HfO_2 by microcontact printing: (c) line scan and (d) Hf Auger electron elemental mapping on the test structure.

densely packed ODTS film capable of completely deactivating the HfO_2 growth, according to Fig. 2. The optimal contact time of 30 s used here imposes a fundamental limitation on the quality of the ODTS layer due to the short formation time. Thus the microcontact-printed ODTS films likely have higher defects compared to those developed from the solution phase. The presence of defects enables the Hf precursor to penetrate through the SAM and nucleate onto the substrate active sites, resulting in the growth of HfO_2 in the ODTS-coated regions [12,32].

Area-selective ALD of Pt using microcontact-printed ODTS was also explored. Whereas a hexagonal pattern was investigated for HfO_2, a rectangular array was used for Pt. After microcontact printing ODTS on YSZ using a 4 μm × 2 μm patterned stamp (generating 4 μm squares of ODTS SAMs separated by 2 μm lines), 33–35 Å Pt thin films were selectively deposited onto the patterned YSZ substrates by atomic layer deposition using $MeCpPtMe_3$ and air as ALD precursors. The results are shown in Figs. 4 and 5.

Fig. 4(a) and (b) shows an SEM image of the micropatterned YSZ substrate before and after area-selective ALD of the Pt thin films, respectively. The contrast inverts in the SEM image of Fig. 4(b) relative to that of Fig. 4(a), indicating that Pt deposition occurs in the regions that are not stamped with ODTS. The rounding of the edges observed in the pattern arises from the photolithography step during the fabrication of the silicon master at these small size scales. In addition to SEM, AES was also used to look at the micropatterned Pt grid structures on YSZ. Fig. 4(c)–(d) illustrates the AES analysis of the patterned mesh structures at high spatial resolution. Auger line scans were used to measure the peak intensity of the Pt and C Auger peaks as a function of position along the defined line displayed in Fig. 4(b). In Fig. 4(c), the Pt, and C spectra clearly show the expected intensity alternation.

AES elemental mapping of Pt was also conducted based on the test pattern. The scanned area is defined in the SEM image in Fig. 4(b). As mentioned earlier, in an AES elemental map, the brightness of the pixel value increased with the Auger peak intensity of the designated element. Fig. 4(d) displays the elemental mapping of Pt, where the bright regions indicate the presence of Pt and the dark areas indicate the absence of Pt. Pt clearly is deposited in the desired grid pattern. Both the SEM image (Fig. 4(b)) and the AES image (Fig. 4(d)) have the same shape, which indicates successful confinement of Pt deposition to the ODTS-free region of the substrate only. Both the results from SEM and AES confirm that the Pt patterns were well defined and directed with high selectivity by the patterned SAMs generated with microcontact printing.

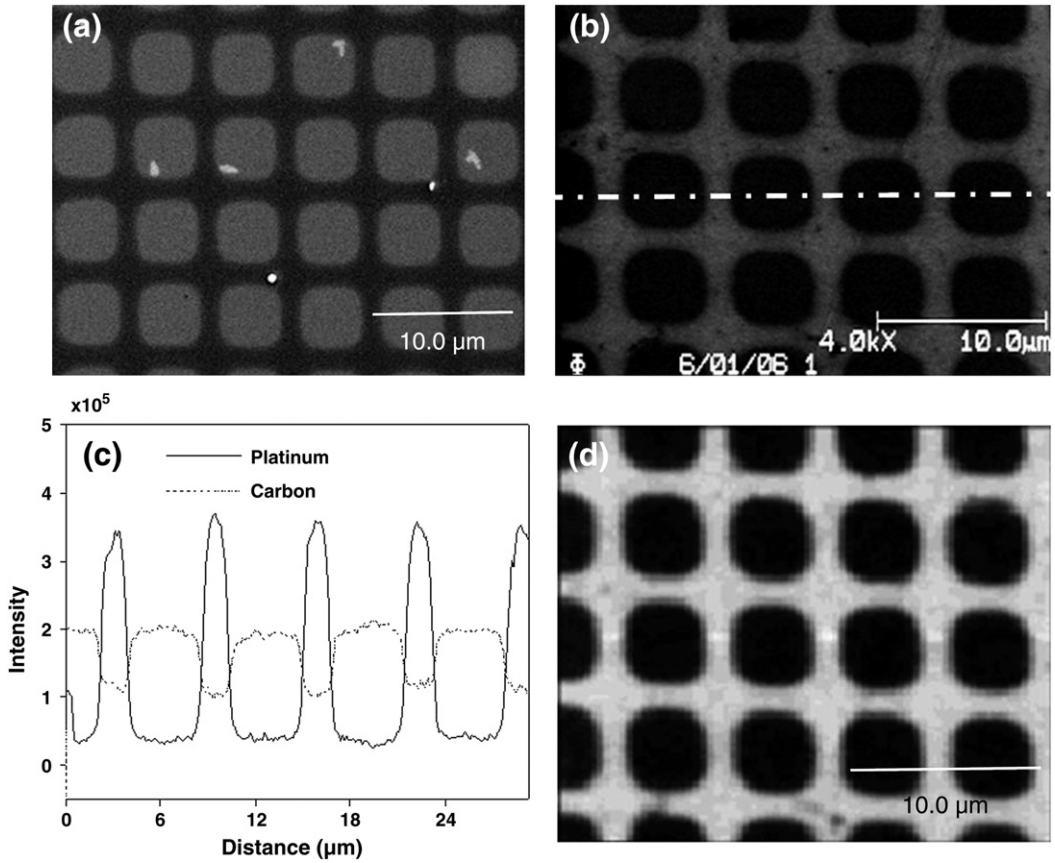

Fig. 4. SEM images of patterned ODTS on YSZ (a) before and (b) after area-selective ALD, respectively. In (a), the brighter squares are where ODTS was stamped. AES analysis on patterned structure after the area-selective ALD of Pt on YSZ by microcontact printing: (c) line scan showing alternation of Pt and C signals and (d) Auger elemental map for platinum on the micropatterned grid structure. Note: in (c), the intensity of the Pt does not go to zero at the ODTS-coated regions because the peak energy used for Pt line scan was 70 eV, which is located on a Zr satellite peak.

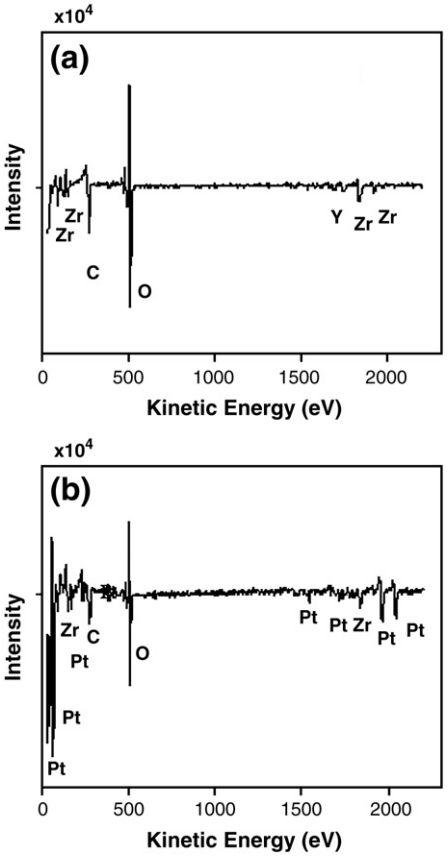

Fig. 5. (a) and (b) are Auger survey spectra of the areas of an ODTS-coated region and an ODTS-free region of YSZ, respectively. The measurements were performed after the Pt ALD exposure.

Furthermore, Auger survey spectra, which provide information on the relative concentrations of elements, were collected in both the ODTS-coated and the uncoated regions of the YSZ substrate with a beam energy of 10keV. The survey spectra, shown in Fig. 5, reveal that in the ODTS-coated YSZ regions (Fig. 5(a)), the Pt signal is below the AES detection limit (<0.1%), whereas, in the ODTS-free YSZ regions (Fig. 5(b)), the Pt at.% is 24%, a value which is comparable to that for non-chemically treated YSZ reference samples in the same ALD run. This result indicates that the Pt thin films are selectively deposited only onto the ODTS-free regions of the substrate and are blocked at the regions coated by ODTS. Note that the observation of signal from the substrate underneath 33–35 Å of Pt may indicate that the Pt film at this thickness is porous, a result which is consistent with previous XRR measurements [17,33].

Differences in the selectivity of the area-selective ALD process for HfO_2 compared to Pt cannot be discerned strictly from the microscopy images. The SEM micrographs of Figs. 3(b) and 4(b) would suggest that selectivity has been achieved for both HfO_2 and Pt. However, elemental analysis carried out by Auger electron spectroscopy reveals clear differences in selectivity between the two materials, and shows incomplete selectivity for HfO_2. The Auger elemental mapping of Hf, plotted in Fig. 3(d), shows evidence for HfO_2 deposition in the ODTS-protected regions, whereas the Pt elemental map shown in Fig. 4(d) has significantly better contrast between the ODTS-coated regions and ODTS-free regions, with no observable Pt signal in the ODTS-coated regions. The observation that higher selectivity is achieved for Pt using microcontact-printed ODTS supports the conclusion, based on Fig. 2, that Pt ALD can be more easily deactivated than HfO_2 ALD.

It is interesting to compare the ALD growth profile at the boundary between the ODTS-coated and ODTS-free regions for area-selective ALD of both HfO_2 and Pt. It is known that for SAMs, the edge of ODTS films will contain a high density of defects in contrast with the interior of the film [47–49]. Thus, it is expected that ALD processes for which the requirement on the quality of the SAM is more severe, such as that for HfO_2, will more readily deposit at these poorly packed interfacial areas compared to processes, such as Pt, which are less sensitive to the quality of the SAM. This analysis suggests that for patterned Pt and HfO_2 fabricated through the soft lithography-based area-selective ALD method, the edge of the Pt pattern should be sharper than the edge for HfO_2. Although we cannot rule out the effect of the different pattern sizes and stamping protocols that were used between the Pt and HfO_2 experiments, the line scan data in Figs. 4(c) and 5(c) do show sharper edges for the Pt pattern. The HfO_2 pattern edges are poorly defined, with a gradient occurring over nearly 10 μm. The Pt pattern edges, by comparison, are relatively sharp on the scale of approximately 1 μm. We note that the lateral resolution of the scanning Auger

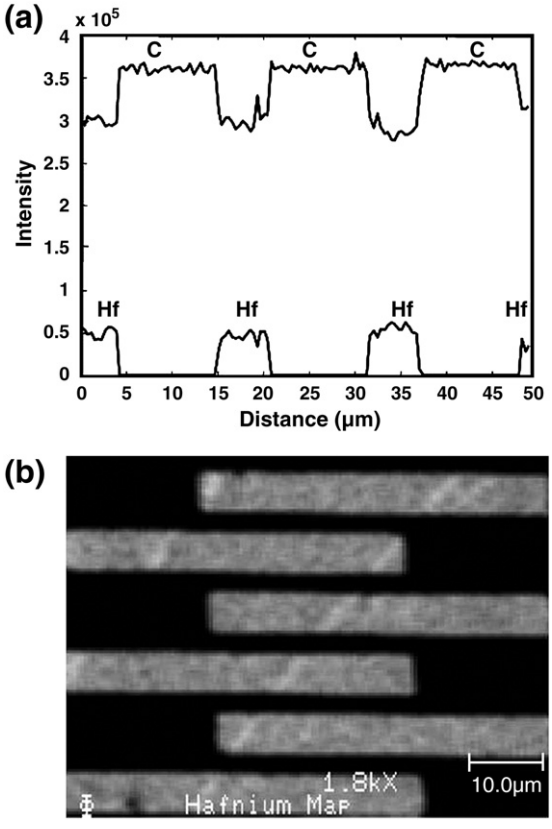

Fig. 6. AES analysis on a patterned SiO_2/Si structure after the area-selective HfO_2 ALD process by selective surface attachment: (a) line scan; (b) Hf Auger electron elemental mapping on the test structure.

is 10nm, which can also be element dependent. However, we can rule out the contribution of element dependent lateral resolution as an explanation for the poorer definition of the HfO_2 edge in this work since in previous studies using area-selective ALD to deposit HfO_2 on photolithographically-patterned SiO_2/Si substrates, the AES line scan of the patterned HfO_2 demonstrated very sharp edges, as discussed below [7,14].

Although the effect is less for Pt, the line scans obtained by Auger analysis of both HfO_2 and Pt (Figs. 3(d) and 4(d), respectively) demonstrate an indistinct interface between deactivated regions and film growth regions. As a comparison, a previous study on area-selective ALD achieved by selective surface modification of a patterned SiO_2/Si substrate demonstrated a sharp interface between deactivated and non-deactivated areas [7]. Fig. 6 below shows the results of Auger studies on the selective surface attachment sample. In that study, the substrate was a patterned SiO_2/Si–H wafer. Based on the intrinsic selectivity of ODTS to SiO_2 over Si–H, only the oxide regions were deactivated. Subsequently, HfO_2 was deposited on non-deactivated Si–H regions. Fig. 6(a) is the line scan for a patterned sample prepared in this way after ALD, and Fig. 6(b) shows the Hf Auger mapping on the patterned area. As shown in Fig. 6(a), the Hf amount is undetectable on the chemically deactivated oxide regions. In contrast, the Hf intensity is clearly detectable for the microcontact-printed sample in Fig. 4(d). We reach the following conclusions. Area-selective ALD achieved by microcontact printing of SAMs is a fast and economical method to define the HfO_2 and Pt growth. However, for excellent pattern definition and spatial resolution, selective surface modification of patterned SiO_2/Si was found to be superior for HfO_2. The reason for the higher selectivity, we believe, is due to the formation of extremely high quality self-assembled monolayers in the latter case [12]. Because the requirements on the SAM resist are not as stringent for Pt ALD (See Fig. 2), the difference in selectivity between microcontact printing and selective surface modification methods may not be as large for Pt.

4. Conclusions

To summarize, HfO_2 and Pt area-selective deposition has been achieved by the combination of microcontact printing and atomic layer deposition. With this method, we observed that a small amount of HfO_2 deposited on the SAM-protected area while Pt growth took place only in the ODTS-free regions. Consequently, area-selective ALD of Pt was observed to have high selectivity and spatial resolution with this method. However, an indistinct edge between the deactivated and non-deactivated regions was observed for both materials. In addition, compared to the selective adsorption method on patterned SiO_2/Si substrates, the selectivity and resolution of the microcontact method used here are poorer for the HfO_2 system. By optimizing and improving the microcontact printing for better SAM transfer, it may be possible to improve the selectivity for HfO_2. On the other hand, there may be fundamental limitations due to the shorter SAM formation time characteristic of the soft lithography process that restrict the ultimate selectivity. Finally, the microcontact printing method of area-selective ALD can be very useful in terms of the speed and cost.

Acknowledgments

This work was supported in part by the NSF/SRC Center for Environmentally Benign Semiconductor Manufacturing, Award No. Q423740, the Stanford Initiative for Nanoscale Materials and Processes, and the Center for Integrated System. The authors would like to thank Prof. Paul C. McIntyre for the use of his ALD reactor, Dr. Hyoungsub Kim for his help on the ALD of HfO_2, and Zhebo Chen for his help with making Fig. 1.

References

[1] M. Ritala, M. Leskelä, Handbook of Thin Film Materials, Academic Press, San Diego, CA, 2002.
[2] M. Ritala, M. Leskelä, E. Rauhala, P. Haussalo, J. Electrochem. Soc. 142 (1995) 2731.
[3] T. Suntola, Mater. Sci. Rep. 4 (1989) 261.
[4] S.M. George, A.W. Ott, J.W. Klaus, J. Phys. Chem. 100 (1996) 13121.
[5] R.L. Puurunen, Chem. Vap. Depos. 9 (2003) 327.
[6] M.J. Biercuk, D.J. Monsma, C.M. Marcus, J.S. Becker, R.G. Gordon, Appl. Phys. Lett. 83 (12) (2003) 2405.
[7] R. Chen, H. Kim, P.C. McIntyre, D.W. Porter, S.F. Bent, Appl. Phys. Lett. 86 (19) (2005) 191910.
[8] J.P. Lee, Y.J. Jang, M.M. Sung, J. Am. Chem. Soc. 126 (2004) 28.
[9] K.J. Park, J.M. Doub, T. Gougousi, G.N. Parsons, Appl. Phys. Lett. 86 (2005) 051903.
[10] P. Packan, Science 285 (2000) 2079.
[11] M.H. Park, Y.J. Jang, H.M. Sung-Suh, M.M. Sung, Langmuir 20 (2004) 2257.
[12] R. Chen, H. Kim, P.C. McIntyre, S.F. Bent, Appl. Phys. Lett. 84 (2004) 4017.
[13] M. Yan, Y. Koide, J.R. Babcock, P.R. Markworth, J.A. Belot, T.J. Marks, R.P.H. Chang, Appl. Phys. Lett. 79 (11) (2001) 1709.
[14] R. Chen, S.F. Bent, Adv. Mater. 18 (2006) 1086.
[15] R. Chen, Ph.D. Thesis, Surface Modification for Area Selective Atomic Layer Deposition on Silicon and Germanium, in Stanford University, (2006).
[16] R. Chen, D.W. Porter, H. Kim, P.C. McIntyre, S.F. Bent, Mater. Res. Soc. Symp. Proc. 917 (2006) E11_05.
[17] X. Jiang, S.F. Bent, Electrochem. Soc. Trans., (in press).
[18] G.D. Wilk, R.M. Wallace, Appl. Phys. Lett. 76 (2000) 112.
[19] L. Kang, Y. Jeon, K. Onishi, B.H. Lee, W.J. Qi, R. Neih, S. Gopalan, J.C. Lee, Dig. Tech. Pap. - Symp. VLSI Technol. 44 (2000).
[20] J. Sinfelt, Catalysts Discoveries, Concepts, and Applications, Wiley, New York, 1983.
[21] S.M. Sze (Ed.), VLSI Technology, 2nd ed., Mc Graw-Hill, New York, 1988.
[22] R.E. Jones, S.B. Desu, MRS Bull. 21 (1996) 55.
[23] U.S. Department of Energy, Fuel Cell Handbook, 7th ed., 2004 Morgantown, West Virginia.
[24] J.P. Lee, Y.J. Jang, M.M. Sung, Adv. Funct. Mater. 13 (11) (2003) 873.
[25] M.M. Sung, Proc., Electrochem. Soc. P2005–09 (2005) 203.
[26] E.K. Seo, J.W. Lee, H. Sung-Suh, M.M. Sung, Chem. Mater. 16 (2004) 1878.
[27] A. Ulman, Chem. Rev. 96 (1996) 1533.
[28] J.D. Swalen, D.L. Allara, J.D. Andrade, E.A. Chandross, S. Caroff, J. Israelachvili, T.J. McCarthy, R. Murray, R.F. Pease, J.F. Rabolt, K.J. Wynne, H. Yu, Langmuir 3 (1987) 932.
[29] G.K. Jennings, P.E. Laibinis, Colloids Surf., A Physichochem. Eng. Asp. 116 (1996) 105.
[30] Y.N. Xia, G.M. Whitesides, Angew. Chem., Int. Ed. Engl. 37 (1998) 550.
[31] M. De Ridder, R.G. Van Welzenis, H.H. Brongersma, Surf. Interface Anal. 33 (2002) 309.

[32] R. Chen, H. Kim, P.C. McIntyre, S.F. Bent, Chem. Mater. 17 (2005) 536.
[33] X. Jiang, S.F. Bent, Submitted for publication.
[34] T. Aaltonen, A. Rahtu, M. Ritala, M. Leskela, Electrochem. Solid-State Lett. 6 (9) (2003) C130.
[35] T. Aaltonen, M. Ritala, T. Sajavaara, J. Keinonen, M. Leskelä, Chem. Mater. 15 (2003) 1924.
[36] T. Aaltonen, M. Ritala, Y.L. Tung, Y. Chi, K. Arstila, K. Meinander, M. Leskela, J. Mater. Res. 19 (2004) 3353.
[37] S.R. Wasserman, Y. Tao, G.M. Whitesides, Langmuir 5 (1989) 1074.
[38] D.K. Schwartz, Annu. Rev. Phys. Chem. 52 (2001) 107.
[39] S.H. Chen, C.W. Frank, Langmuir 5 (1989) 45.
[40] G.J. Sagiv, J. Colloid Interface Sci. 112 (1986) 457.
[41] D.L. Allara, R.G. Nuzzo, Langmuir 1 (1985) 45.
[42] W.A. Zisman, Adhesion and Cohesion, Elsevier, New York, 1962.
[43] A.S. Killampalli, P.F. Ma, J.R. Engstrom, J. Am. Chem. Soc. 127 (17) (2005) 6300.
[44] A. Sinha, D.W. Hess, C.L. Henderson, J. Electrochem. Soc. 153 (5) (2006) G465.
[45] A. Sinha, D.W. Hess, C.L. Henderson, Electrochem. Solid-State Lett. 9 (11) (2006) G330.
[46] K.S. Park, E.K. Seo, Y.R. Do, K. Kim, M.M. Sung, J. Am. Chem. Soc. 128 (3) (2006) 858.
[47] R.B.A. Sharpe, B.J.F. Titulaer, E. Peeters, D. Burdinski, J. Huskens, H.J.W. Zandvliet, D.N. Reinhoudt, B. Poelsema, Nano Lett. 6 (6) (2006) 1235.
[48] A.J. Black, K.E. Paul, J. Aizenberg, G.M. Whitesides, J. Am. Chem. Soc. 121 (1999) 8356.
[49] J. Aizenberg, A.J. Black, G.M. Whitesides, Nature 394 (1998) 868.